Journal of Hydroscience and Hydraulic Engineering
Vol. 19, No.2 November, 2001, 71-83

STUDY ON CHARACTERISTICS OF RESERVOIR SEDIMENTATION WITH HYDRAULIC JUMP

By

Koichi Suzuki and Akihiro Kadota

Department of Civil and Environmental Engineering, Ehime University, Matsuyama, Japan

and

Bal B. Parajuli

Graduate School of Science and Engineering, Ehime University, Matsuyama, Japan

SYNOPSIS

The bed profile of sediment deposition in a reservoir in mountain rivers with steep slopes, like in Nepal, is characterized by the water level profile with a hydraulic jump. The process of sediment deposition was studied in a steep laboratory flume with a dam of a small height, which causes the hydraulic jump in the reservoir. Starting at the critical section of the hydraulic jump, the deposition of sediment progressed towards the dam as the flow velocity decreased and the hydraulic jump shifted upwards. The bed configurations were found to be two-dimensional and three-dimensional in experiments with coarse and fine sediment, respectively. The average bed profiles and water depths were numerically well simulated by applying one-dimensional continuity equations of flow and sediment transport and considering the step length and pickup rate of the sediment particles.

INTRODUCTION

The characteristics of the bed profile of reservoir sedimentation in mountain rivers with steep slopes, like in Nepal, depend on the water level profile with the hydraulic jump. "The sediment deposition pattern in the reservoir, as a delta form, can reflect the transport process in the reservoir and its delivery and distribution process" (4). The process of sediment deposition was studied experimentally by using the coarse and fine sediment in a small and steep laboratory flume with a model dam, which causes the hydraulic jump in the reservoir. As the flow velocity decreases towards the downstream side of the hydraulic jump section, the sediment deposition starts in a steep channel in the subcritical region moving towards both the dam and the upstream. Two-dimensional and three-dimensional temporal variations in bed levels were found in experiments with coarse and fine sediment, respectively. Lastly, the average bed profiles were numerically simulated with the continuity equations of one-dimensional flow and sediment, and at the same time taking into consideration the shift of the location of the hydraulic jump.

EXPERIMENTAL STUDY FOR THE SEDIMENT DEPOSITION PROCESS

Summary of the Experiment

The process of sediment deposition in a steep slope reservoir was studied experimentally in the

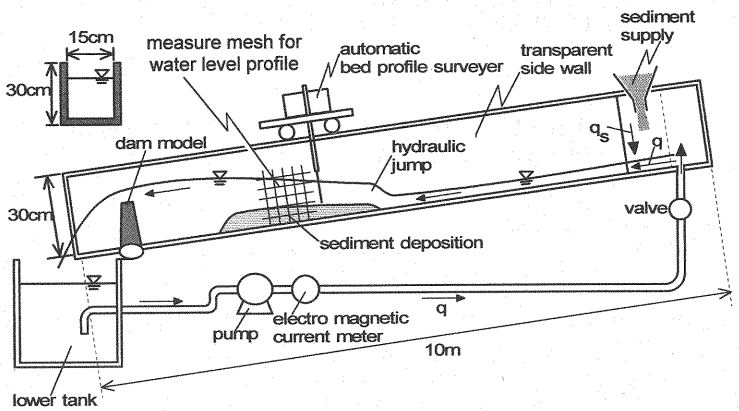

Fig. 1 Flume Channel and Experimental Equipment

Table 1 Experimental Conditions

Runs	Sediment Size (mm)	Discharge q (cm^2/s)	Dam height W(cm)	Channel slope	Normal depth h_0(cm)	Froude number F_{r0}	Sediment supply q_{Bin}(cm^2/s)
A	2.5	200	10	0.02	2.7	1.44	0.111
B	2.5	266	10	0.02	2.8	1.81	0.089
C	2.5	333	10	0.02	3.2	1.86	0.105
D	2.5	200	7	0.02	2.5	1.62	0.113
E	2.5	266	7	0.02	2.7	1.91	0.111
F	2.5	333	7	0.02	3.0	2.05	0.111
G	0.13	200	10	0.02	2.2	1.96	0.036
H	0.13	266	10	0.02	3.0	1.63	0.031
I	0.13	333	10	0.02	3.7	1.49	0.033
J	0.13	333	7	0.02	3.7	1.49	0.038

laboratory flume as shown in Fig. 1, for both fine and coarse sediment under various conditions of flow discharge, dam height, and sediment supply. The experimental flume with a rectangular section was 10m long, 0.15m wide, and 0.30m deep, which could be adjusted for different slopes. A model dam was built at the downstream end of the flume. An electronic profile indicator with a depth-recording gauge was connected to a data recorder, which moved throughout the flume. Measurements of the bed profiles and water levels along the channel were arranged precisely.

Various experimental conditions were adopted. The size of sediment, dam height, water discharge, and the amount of sediment supply are shown in Table. 1. Two different sizes (d) of sediments were used: fine sediment of 0.13mm size and coarse sediment of 2.5mm size. Two types of dam height (W) of 7cm and 10 cm were made. Three different water discharges per unit width (q) of 200, 266, and 333$cm^3/s/cm$ were used. Supplies of sediment (q_{Bin}) were constant: about 0.1$cm^3/s/cm$ in the experiment with coarse sediment and 0.03 $cm^3/s/cm$ in the experiment with fine sediment. The slope of the channel was exactly 1/50. Manning's roughness coefficients were computed to be 0.013 for the supercritical flow region of upstream side, where there was no sediment deposition, and 0.03 for the subcritical flow region, where the sediment deposition occurred.

The water levels and deposition profiles of sediments were measured for each experimental Run at an interval of 30 minutes and at every 10 cm along the channel starting from the dam. The rectangular channel was fixed properly in the required slope. The discharge of water and the amount

of sediment were supplied at a constant rate from the upstream end of the flume, which were controlled by means of a computer and a hopper, respectively. The water level along the channel was measured manually with a mesh scale drawn on the transparent sidewall of the flume. The temporal variations of the bed levels were recorded precisely with an electronic profile indicator in terms of voltage, which later was calibrated in a proper unit.

The profiles of the longitudinal deposition pattern were measured in three locations, that is, along the left sidewall, the right sidewall, and at the center of the channel. However, the deposition profiles in a lateral direction were observed to be almost uniform for coarser sediments in contrast to the three-dimensional profiles for finer sediments.

The Phenomenon of Sediment Deposition with the Hydraulic Jump

To observe the phenomenon of sedimentation in a reservoir in a steep slope, a hydraulic jump, which characterizes the profiles of deposition, was formed in the flume. A constant rate of sediment was fed from the upstream end. Moreover, there was no deposition in the supercritical region upstream of the hydraulic jump. Because of the greater water depth in the subcritical region downstream of the jump, flow velocity was reduced and the deposition of sediment started.

The process of sedimentation is schematically illustrated as in Fig. 2. Initially, a fully developed hydraulic jump occurred. As the sediment deposition started, it advanced rapidly to the downstream side of the section of the hydraulic jump, but at slower rate to the upstream side. The flow over the jump then formed surface waves. This wavy jump became a full hydraulic jump again with some more deposition of sediment. The location of the hydraulic jump also shifted upwards from the initial position with an occurrence of the sediment deposition in the subcritical section, which was also reported by Matsushita (3). The phenomenon of a stable and unstable hydraulic jump of surface waves was occurred repeatedly in the steep channel reservoir during the sediment deposition. This phenomenon can be summarized as follows:

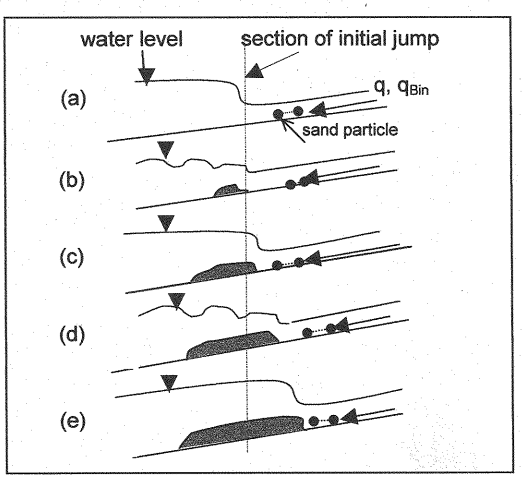

Fig. 2 Schematic figure of upward movement of the hydraulic jump

After feeding the sediment with water discharge from the upstream end, the sediment started to deposit. At this stage, the hydraulic jump (a) becomes a wavy jump (b). This wavy jump again becomes a full hydraulic jump (c) with the progress of deposition moving in an upward direction. However, the position of this hydraulic jump shifts to the upstream side of initial one (a). Regarding the continuous sediment deposition, the full jump (c) again starts to be a wavy jump (d), which later becomes as a full jump (e) with the upward movement from the previous position.

Configuration of the Sediment Deposition and Bed Profiles

The bed forms of the sediment deposition in the experiment with larger sediment were found to be two-dimensional, i.e., the depth of deposition varied only along a longitudinal direction and was uniform in a transverse direction. On the other hand, bed forms of the sediment deposition were

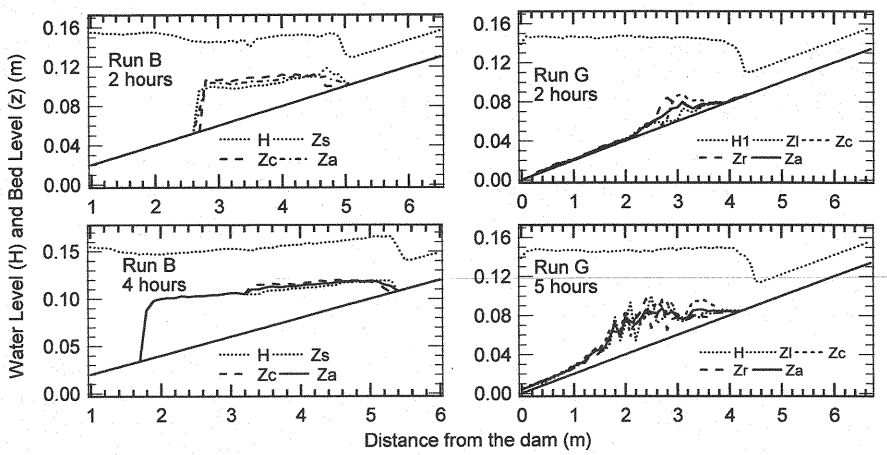

Fig. 3 Typical observed profiles of two-dimensional and three-dimensional bed variations of sediment deposition

found to be three-dimensional with the sand waves in the case of fine sediment, where the deposition configuration was also found to vary along a transverse direction at all sections of the channel.

Typical observations of the two-dimensional bed profiles in coarse sediment and three-dimensional bed profiles in fine sediment and their averages are shown in Fig. 3. In this figure, Zs, Zc, and Za represent the bed levels along both sidewalls and at the center of the channel, and their average, respectively in coarse sediment. Zl, Zr, Zc, and Za represent the longitudinal bed profiles on the left side, right side, center of the channel, and their average in fine sediment, respectively. The water surface profile for each respective time is represented by H. Fig. 4 shows the temporal variations of water surface (H) and bed profiles (Z) averaged over three longitudinal lines for both larger and smaller size of the sediment, where sub suffixes represent the times in hour. The deposition of sediment starts from just downstream of the hydraulic jump section, and progresses both towards the dam rapidly and upwards slowly. With the development of deposition, the location of the hydraulic jump shifts to the upstream side from its previous position. It was observed that the upward speed of advancement of deposition in the case of larger size of sediment is comparatively faster than in the case of a smaller size of sediment.

The bed profiles observed showed that sediment depositions were in the form of a delta deposition in the case of coarse sediment and a tapering deposition in the case of fine sediment, as shown in Fig. 4. The position of the hydraulic jump was found to have shifted upwards rapidly in the experiment with coarse sediment where the sediment pattern is two-dimensional in the form of delta. But the position of the hydraulic jump shifted upwards from its initial position very slowly in the case of fine sediment, where the tapering form of sediment deposition occurs.

NUMERICAL SIMULATION

The sediment deposition in the reservoir with a steep channel is calculated by means of a hydraulic jump. One-dimensional continuity equation for water and the energy equation are used to calculate the water levels. Similarly, the equation of sediment transport and the continuity equations for sediment are used to calculate the bed levels.

Basic Equations for One-dimensional Analysis

For the sake of simplicity, flow is considered one-dimensional, that is, the depth varies along the longitudinal direction (x-axis) only. In this regard, a one-dimensional flow equation is applied to

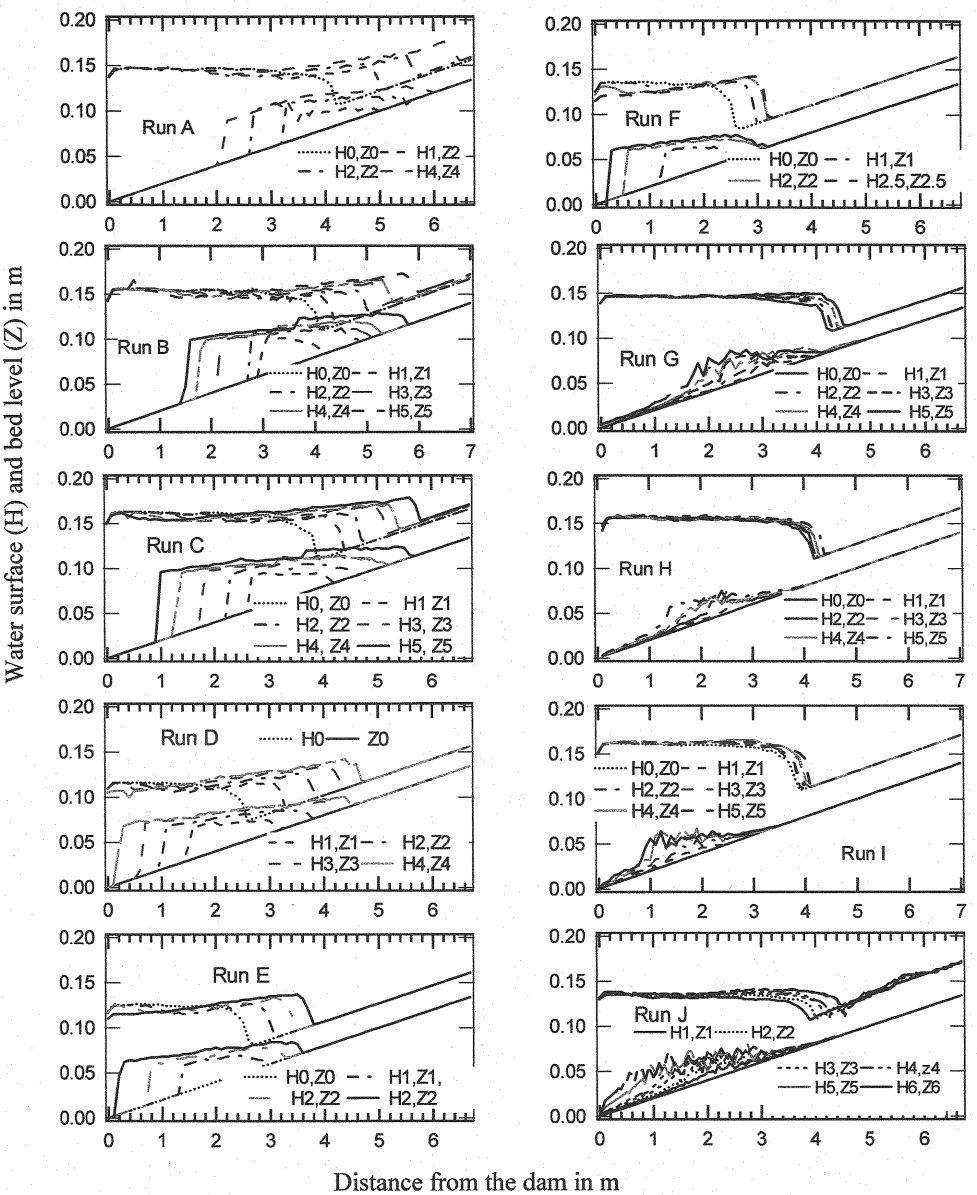

Fig. 4 Typical observed temporal variations of the bed profiles and water surface

calculate the water depth, and the bed variation corresponding to the flow is analyzed by one-dimensional continuity equations.

The one-dimensional energy equation and continuity equation for the steady flow, respectively are expressed as follows:

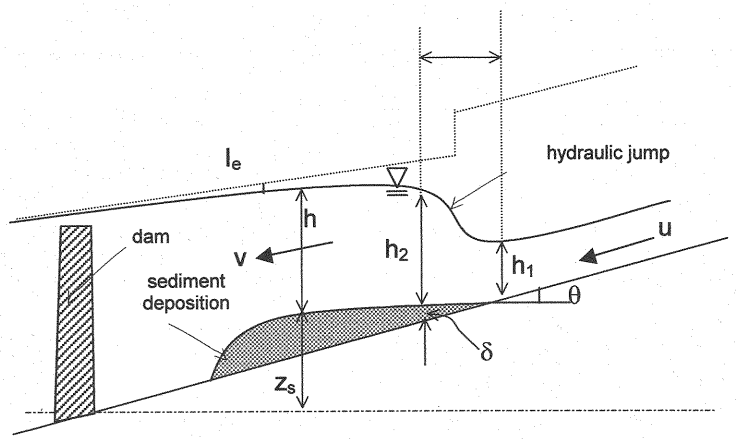

Fig. 5 Notations and definitions

$$\frac{\partial}{\partial x}\left(z_s + h\cos\theta + \frac{\alpha v^2}{2g}\right) = -I_e; \quad q = vh \tag{1}$$

where v is the average flow velocity of the cross section, z_s is the bed level above the reference level, q is the water discharge per unit width, h is the water depth, θ is the angle of the bed slope, α is the coefficient of energy, g is the acceleration due to gravity, and $I_e=n^2v^2/R^{4/3}$ is the energy gradient, where n is the Manning's roughness coefficient, and R is the hydraulic radius of the section of the channel.

The channel has a steep slope and the upstream flow is supercritical. The backwater effect originating from the dam will extend to the section of the hydraulic jump. The flow upstream from the jump is governed entirely by the upstream condition. As shown in Fig. 5, the hydraulic jump occurs at the section of the channel where the following Eq.(2) of conservation of momentum equation is satisfied between two sections:

$$\frac{h_2}{h_1} = \frac{\sqrt{1+8G_1^2}-1}{2} \tag{2}$$

where $G_1^2 = F_{r1}^2 / \{\cos\theta - K_j L_j \sin\theta/(h_2 - h_1)\}$ and $F_{r1} = v_1/\sqrt{gh_1}$, h_1 is the flow depth before the jump, h_2 is the flow depth after the jump, v_1 is the flow velocity in upstream before the formation of jump, L_j is the length of the jump (=6(h_2-h_1) by Smetana), K_j is the modified coefficient (≈ 1.0), and θ is the angle of slope.

When the sediment deposition occurs just downstream from the hydraulic jump and a step with the height δ is formed as shown in Fig. 6. The following momentum equation is obtained by Hasegawa (2):

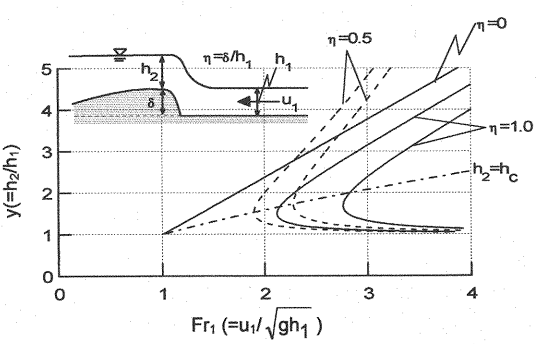

Fig. 6 Conjugate Depths at Hydraulic Jump in Step

$$y^3 + 2\eta y^2 - \left(2F_{r1}^2 + 1 - \eta^2\right)y + 2F_{r1}^2 = 0 \tag{3}$$

where $y=h_2/h_1$, $\eta=\delta/h_1$, and $F_{r1} = u_1/\sqrt{gh_1}$. For $\eta>0$ (step) and $F_{r1}>1$, the relationship between y and F_{r1} expressed by Eq.3 are shown in Fig. 6.

By determining and applying the boundary conditions, the subcritical flow depth can be calculated from downstream to upstream, if the flow depth at the downstream end is known. The supercritical flow depth can be calculated from upstream, if the flow depth at the upstream end is known. Flow depths from downstream and upstream are connected through the hydraulic jump.

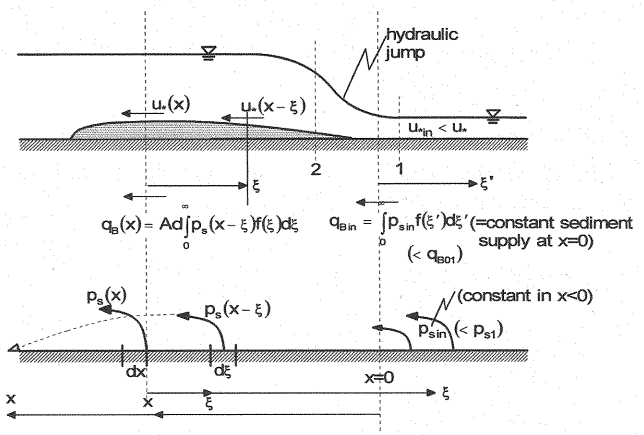

Fig. 7 Schematic Figure Showing Sediment Discharge with a Pick-up Rate p_s and Probability Density Function $f(\xi)$ of the Step Length

In the case where the stream wise pressure gradient is $(\partial h/\partial x \neq 0)$, the local shear velocity u_* should be given by modifying the normal shear velocity u_{*0} as follows:

$$\frac{v}{u_{*0}} = 6.0 + 5.75\log\left(\frac{h}{k_s}\right); \qquad u_* = \frac{u_{*0}}{1+\beta(\partial h/\partial x)} \tag{4}$$

where β is the coefficient to be determined experimentally, v is the average flow velocity over the section ($=q/h$), h is the flow depth, q is the flow discharge of water per unit width at the section, and k_s ($\approx kd$, k: constant) is the equivalent roughness.

The Equation of continuity of sediment can be written as follows:

$$\frac{\partial z_s}{\partial t} + \frac{1}{(1-\lambda)B}\frac{\partial(q_B B)}{\partial x} = 0 \tag{5}$$

where t is time, λ is the porosity of the sediment, B is the width of the river bed, q_B is the sediment discharge per unit width of the river bed.

Suzuki (1981) applied the probabilistic theory of sand movement starting from Einstein (1950) to deal with the local scour phenomenon around a bridge pier in the state of non-equilibrium sediment transport (5), and the term $\partial q_B/\partial x$ given by Eq.10 was derived as follows:

The phenomenon of sliding, jumping and the rolling of sediment particles in a step length, also known as saltation, can be treated by using the probabilistic method. The probability density function of step length, is given by Yano et al. (1968):

$$f(\xi) = (1/L)\exp(-\xi/L); \qquad L = \lambda_1 d \tag{6}$$

where L is the mean step length of the sediment particles, λ_1 is the coefficient (≈ 100 is adopted) as suggested by Einstein (1), and d is the average size of the sediment particles.

Considering the small control section Δx, as shown in Fig. 7, the deposition ratio in Δx of the sediment from the upstream side of the hydraulic jump is given by:

$$Ad\int_{x}^{\infty} p_{sin}(x-\xi)\cdot f(\xi)\cdot d\xi\cdot\Delta x \tag{7}$$

where A is the constant ($=k_3d^3/k_2d^3\approx 2/3$).

The deposition rate in Δx of the sediment picked up from the downstream side of the hydraulic jump is calculated as follows:

$$Ad\int_{0}^{x} p_s(x-\xi)\cdot f(\xi)\cdot d\xi\cdot\Delta x \tag{8}$$

The sediment picked up from the control section (Δx) can be calculated as given by:

$$Adp_s(x)\cdot\Delta x \tag{9}$$

In Eqs. (7), (8), and (9), p_{sin} is the pick-up rate of sediment at the upstream side, $p_s(x\text{-}\xi)$ is the pick-up rate at a section (x-ξ), and $p_s(x)$ is the pick-up rate of sediment transport from the section Δx.

By applying the conservation of sediment discharge, the deposition of sediment in the control section can be written by deducting Eqs.(7) and (8) from Eq.(9) as below:

$$\frac{\partial q_B}{\partial x}=Ad\left\{p_s(x)-\int_0^x p_s(x-\xi)\cdot f(\xi)\cdot d\xi-\int_0^\infty p_{sin}\cdot f(\xi)\cdot d\xi\right\} \tag{10}$$

By definition, these pick-up rates can be rewritten as follows:

$$p_s(x)=\frac{q_{B0}(x)}{A\cdot d\cdot L};\quad p_s(x-\xi)=\frac{q_{B0}(x-\xi)}{A\cdot d\cdot L};\quad p_{sin}=\frac{q_{Bin}}{A\cdot d\cdot L} \tag{11}$$

where q_{B0} is the discharge of equilibrium sediment transport and q_{Bin} is the rate of sediment fed from the upstream of the hydraulic jump.

Comparing the Eqs.(5), (10), and (11), sediment deposition in a small distance Δx of the control section is given by:

$$\frac{\partial z_s}{\partial x}+\frac{1}{1-\lambda}\frac{1}{L}\left\{q_{B0}(x)-\int_0^x q_{B0}(x-\xi)\cdot f(\xi)\cdot d\xi-\int_0^\infty q_{Bin}f(\xi)\cdot d\xi\right\}=0 \tag{12}$$

If the sediment is assumed to be transported as bed load, Meyer-Peter and Müller's equation for the sediment transport may be applied as follows:

$$\frac{q_{B0}}{\sqrt{sgd^3}}=K(\tau_*-\tau_{*c})^m \tag{13}$$

where s ($=\sigma/\rho$-1) is the submerged relative density of the sediment,σ is the density of sediment, ρ is the density of water, d is the sediment size, $\tau_*\left(=u_*^2/sgd\right)$ is the dimensionless shear stress, u_* is the shear velocity, $\tau_{*c}(\approx 0.047)$ is the dimensionless critical shear stress, K (=8), and m (=3/2) are the constant coefficients.

Simulated Profiles of Bed Variation and Water Surface with Observed Ones

The observed bed profiles averaged over three longitudinal lines and water levels were compared with simulated ones for each experiment. Typical comparisons of temporal variations of water surface and bed level are shown in Fig. 8(a) and 8(b), where H and Z represent the water level and bed level, respectively. The average of observed bed profiles and water surface profiles coincided approximately with the simulated ones.

The progression of deposition of simulated and observed bed profiles were compared. Initially, the deposition of sediment was observed just below the section of the hydraulic jump. Typical cases of progressive sediment deposition upwards and downwards, and the upward advancement of the hydraulic jump are as shown in Fig. 9. The edges of the progression of the sediment deposition in downstream and upstream are represented by Ds and Us, respectively and the position of the

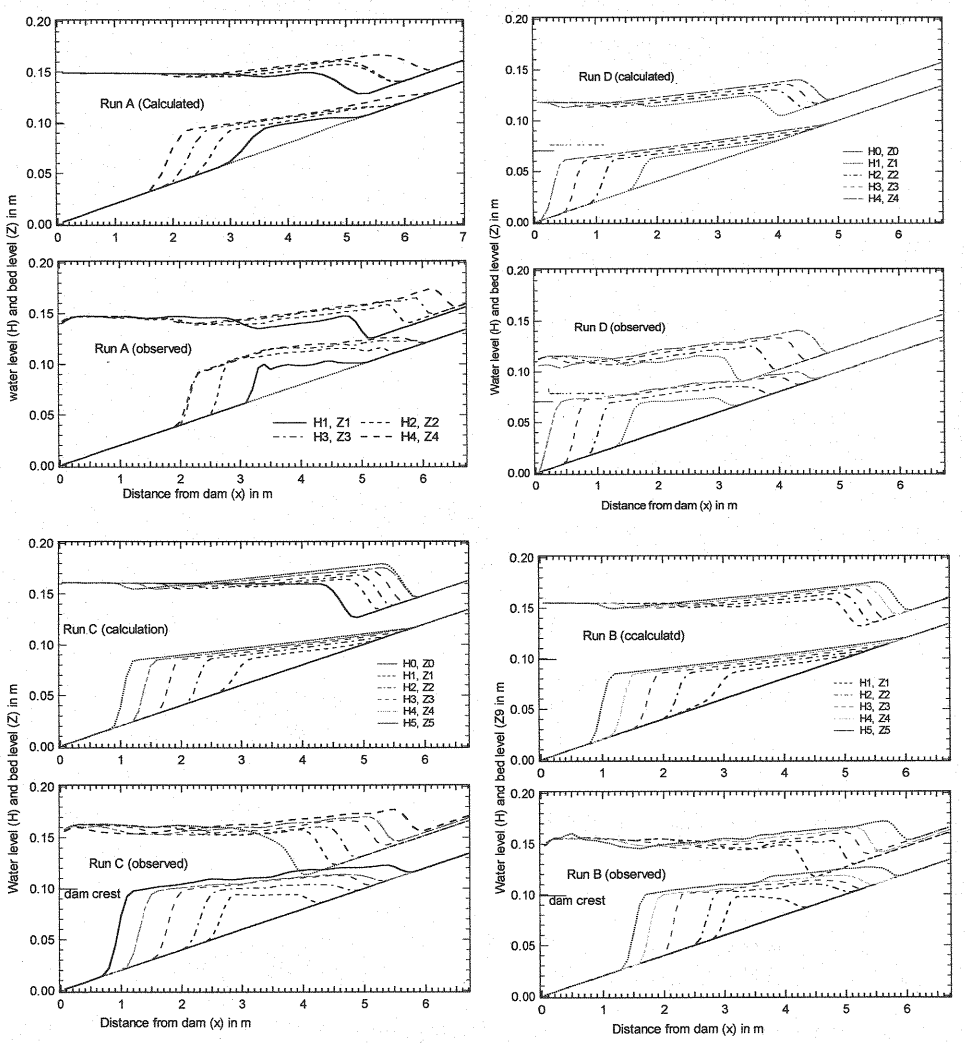

Fig. 8(a) Observed and calculated temporal variations of water surface and averaged bed profiles for coarse sediment

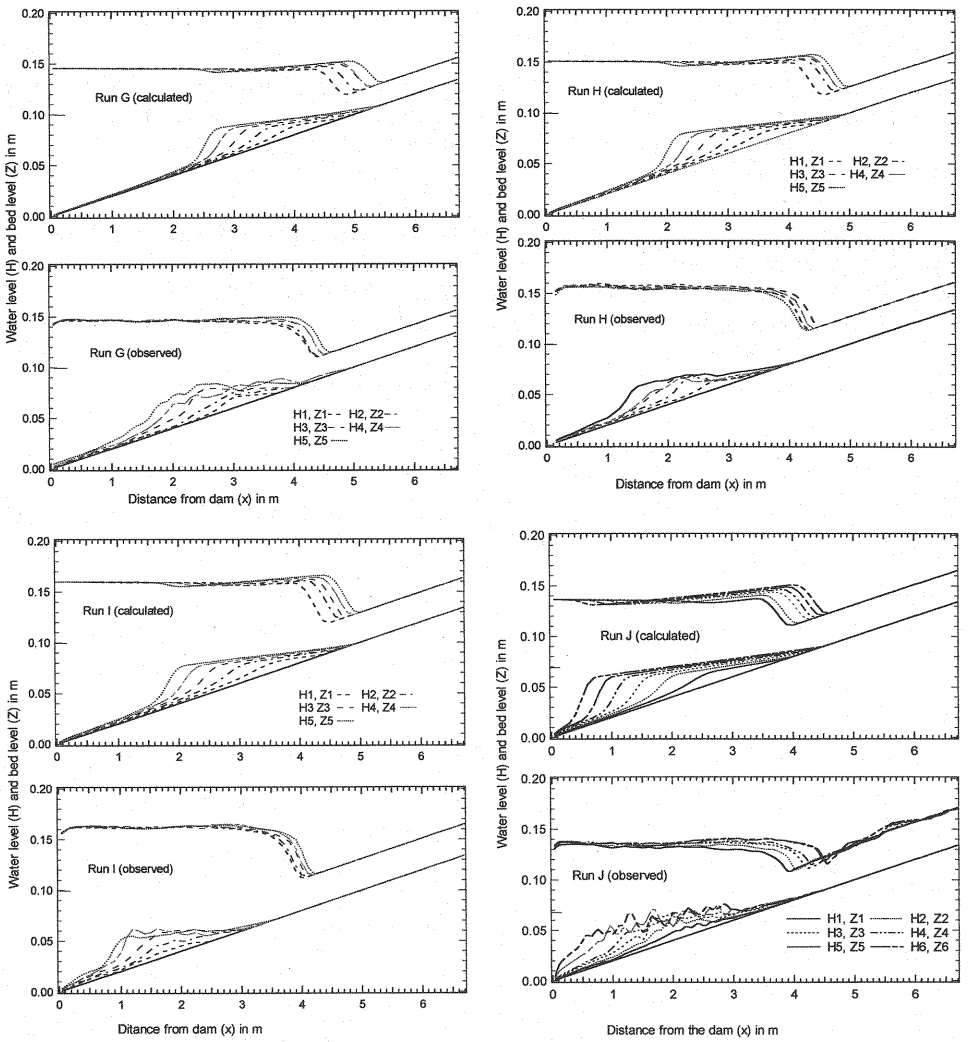

Fig. 8(b) Observed and calculated temporal variations of water surface and averaged bed profiles for fine sediment

hydraulic jump is represented by Hj. The letters (o) and (c) stand for the observed and calculated values, respectively. It was observed that the deposition moved downstream rapidly and upstream slowly in all Runs. The upward movement of sediment deposition in the experiment with fine sediment was found to be much slower than in the experiment with coarse sediment. The observed downstream edges (Ds) and upstream edges (Us) of sediment deposition were compared with the simulated edges of deposition, and they were found to have coincided. Similarly, the upward advancements of the hydraulic jump during deposition, which was also reported by Hasegawa (2), were observed in all runs, and were compared with the simulated positions of the hydraulic jumps. The simulated and observed positions of the hydraulic jump was found to have shifted upwards during the progression of sediment deposition.

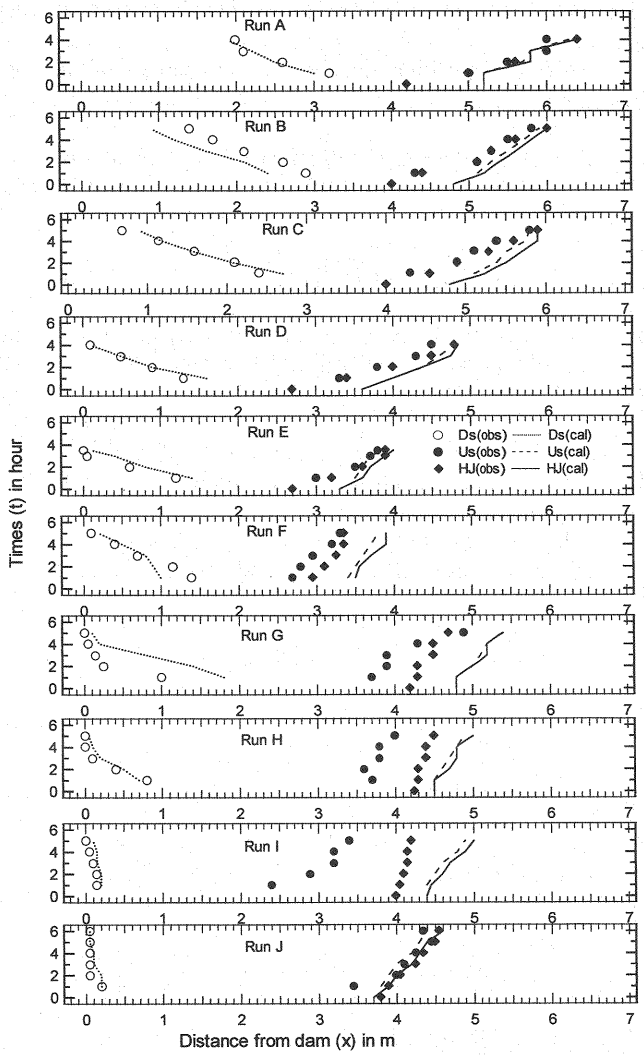

Fig. 9 Observed and calculated positions of the hydraulic jump and the downstream and the upstream edges of the sediment deposition

CONCLUSIONS

Findings of this research show that the bed profile of deposition for fine sediment is three-dimensional with sand waves. The longitudinal bed profile along the two sidewalls and the center of the channel is irregular. However, the bed profiles of coarse sediment are two-dimensional. The profiles of sediment deposition in both cases for fine sediment (average profiles of three longitudinal lines) and larger sediment can be simulated easily by a one-dimensional analysis by means of a hydraulic jump.

The deposition of sediment starts from just below the downstream section of the hydraulic jump.

Also, it progressively moves towards the dam and gradually upwards in a tapering form in the case of fine sediment. However, it moves rapidly upwards, and moves slowly towards the dam as a delta form in the case of coarse sediment.

Due to these patterns of sediment deposition, the upward movement of the location of the hydraulic jump from its previous position is rapid in the case of coarse sediment and very slow in the case of fine sediment.

Due to the fact that the mountain riverbed is a consistent of mixture of sand and gravel, the deposition pattern of sediment for each grain size should be taken into consideration in further research.

REFERENCES

1. Einstein, H.A. : The bed-load function for sediment transportation in open channel flow, U.S. Department of Agriculture, Soil Conservation Service, Technical Bulletin, No.1026, pp. 1-71, 1950.
2. Hasegawa, K. : Bed configurations and flows in mountain rivers, Proceedings of the 33rd Summer Seminar on Hydraulic Engineering, JSCE, A8, pp.1-22, 1988 (in Japanese).
3. Matsushita, F. : Back sand phenomenon in steep slope river –case of rectangular section, straight river, Trans. JSDRE, No.66, pp.48-54, 1976 (in Japanese).
4. Morris, G.L. and J. Fan : Sediment Deposits in Reservoir- Reservoir Sedimentation Handbook, Design and Management of Dams, Reservoirs, and Watersheds for Sustainable Use, McGraw Hill Publication, pp.10.1-10.9, 1997.
5. Suzuki, K. : Study on the clear water scour around a cylindrical bridge pier, Proceedings of the JSCE, No.313, pp.47-53, 1981 (in Japanese).

APPENDIX - NOTATION

The following symbols are used in this paper:

A	= constant ($= k_3 d^3 / k_2 d^3 \approx 2/3$) as defined in Eq.7, 8 and 9;
B	= width of the river bed;
d	= size of sediment;
F_{r1}	= Froud number at the normal flow ($= u_1 / \sqrt{gh_1}$);
G_1	= $F_{r1}/\{\cos\theta - K_j L_j \sin\theta/(h_2-h_1)\}^{0.5}$;
g	= acceleration due to gravity;
H	= water level in all Figures;
h	= flow depth;
I_e	= energy gradient;
K	= constant coefficient in Eq. 13;
k_s	= equivalent roughness coefficient ($\approx kd$, k: constant) in Eq. 4;
K_j	= modified coefficient (≈ 1.0) around the hydraulic jump;
L	= mean step length of the sediment particles;
L_j	= length of the hydraulic jump (=6 (h_2-h_1) by Smetana);
m	= constant coefficient in Eq. 13;
n	= Manning's roughness coefficient;
p_{sin}, $p_s(x-\xi)$, $p_s(x)$	= pick-up rates of sediment as defined by the Eq. 11;
q	= water discharge per unit width;
q_{B0}	= discharge of equilibrium sediment transport;
q_{Bin}	= rate of sediment fed from the upstream of the hydraulic jump;
R	= hydraulic radius of the section of the channel;
t	= time as defined by Eq. 5;

u_1 = Normal flow velocity;
u_*, u_{*0} = local shear velocity and modified normal shear velocity, respectively;
v = average flow velocity of the cross section;
W = dam height;
x = longitudinal direction in Eq. 1;
y = ratio of two conjugate depths at the section of hydraulic jump as defined in Fig. 6;
Za = average of Zl, Zc, and Zr or of Zs and Zc in Figs. 3 and 4;
Zl, Zc, Zr, Zs = bed levels in the left sidewall, at the center, and in the right sidewall, and bed level in both sidewalls, respectively in Figs. 3 and 4;
z_s = bed level above the reference level in Eq. 1;
α = coefficient of energy;
β = coefficient to be determined, experimentally;
δ = change in depth of the sediment deposition in Fig. 5;
η = δ/h_1;
θ = angle of slope of the channel;
λ porosity of the sediment;
λ_1 = coefficient (≈ 100) as suggested as defined Eq. 6;
ρ = density of water;
σ = density of sediment;
τ_* = dimensionless shear stress (u_*^2/sgd);
τ_{*c} = dimensionless critical shear stress ($\approx$0.047); and
ξ = axis of probability density function f(ξ) as defined in Fig. 7.

(Received July 16, 2000 ; revised May 10, 2001)